Author Manuscript

Author Manuscript

Author Manuscript

Author Manuscript

HHS Public Access

Author manuscript

J Alzheimers Dis. Author manuscript; available in PMC 2017 July 06.

Published in final edited form as:

J Alzheimers Dis. 2016 July 6; 53(4): 1499–1516. doi:10.3233/JAD-151179.

High-throughput screening for identification of blood-brain barrier integrity enhancers: a drug repurposing opportunity to rectify vascular amyloid toxicity

Hisham Qosa[1], **Loqman A. Mohamed**[1], **Sweilem B. Al Rihani**[1], **Yazan S. Batarseh**[1], **Quoc-Viet Duong**[1], **Jeffrey N. Keller**[2], and **Amal Kaddoumi**[1,*]

[1]Department of Basic Pharmaceutical Sciences, School of Pharmacy, University of Louisiana at Monroe, Monroe, LA, USA

[2]Pennington Biomedical Research Center, Louisiana State University, Baton Rouge, LA, USA

Abstract

The blood-brain barrier (BBB) is a dynamic interface that maintains brain homeostasis and protects it from free entry of chemicals, toxins and drugs. The barrier function of the BBB is maintained mainly by capillary endothelial cells that physically separate brain from blood. Several neurological diseases, such as Alzheimer's disease (AD), are known to disrupt BBB integrity. In this study, a high-throughput screening (HTS) was developed to identify drugs that rectify/protect BBB integrity from vascular amyloid toxicity associated with AD progression. Assessing Lucifer Yellow permeation across *in-vitro* BBB model composed from mouse brain endothelial cells (bEnd3) grown on 96-well plate inserts was used to screen 1280 compounds of Sigma LOPAC®1280 library for modulators of bEnd3 monolayer integrity. HTS identified 62 compounds as disruptors, and 50 compounds as enhancers of the endothelial barrier integrity. From these 50 enhancers, 7 FDA approved drugs were identified with EC_{50} values ranging from 0.76–4.56 μM. Of these 7 drugs, five were able to protect bEnd3-based BBB model integrity against amyloid toxicity. Furthermore, to test the translational potential to humans, the 7 drugs were tested for their ability to rectify the disruptive effect of Aβ in the human endothelial cell line hCMEC/D3. Only 3 (etodolac, granisetron and beclomethasone) out of the 5 effective drugs in the bEnd3-based BBB model demonstrated a promising effect to protect the hCMEC/D3-based BBB model integrity. These drugs are compelling candidates for repurposing as therapeutic agents that could rectify dysfunctional BBB associated with AD.

Keywords

High-throughput screening; blood–brain barrier; permeability; repurposing; Amyloid-β

*Corresponding Author: Amal Kaddoumi (kaddoumi@ulm.edu), Department of Basic Pharmaceutical Sciences, School of Pharmacy, University of Louisiana at Monroe, 1800 Bienville Dr., Monroe, LA 71201. Phone 318-342-1460; Fax 318-342-1737.

Author Manuscript Author Manuscript Author Manuscript Author Manuscript

Introduction

The blood-brain barrier (BBB) is a complex barrier that separates brain from blood. BBB comprises of different cellular components however, the barrier or gate function of the BBB is provided primarily by the endothelial cells (ECs) lining the brain capillaries [1, 2]. These ECs are anchored to a continuous basement membrane (BM) and connected to each other by tight and adherens junctions [3]. Tight junctions (TJ) between adjacent ECs face the luminal side of the BBB, and consist of the transmembrane TJ proteins occludin, claudins and junctional adhesion molecules (JAMs), and adaptor molecules that connect TJ proteins to actin cytoskeleton [1, 4]. Similarly, adherens junctions (AJ) face the abluminal side of the BBB, and consist of the transmembrane AJ proteins VE-cadherin and catenin, and adaptor molecules that link AJ proteins to actin cytoskeleton [1, 4]. Thus, sealed ECs monolayer form a restrictive barrier that precludes free movement of substances between blood and brain.

Several lines of evidence implicate that disruption of the BBB may precede, accelerate, or contribute to neuronal dysfunction [5]. Moreover, the compromised BBB is associated with several neurological diseases such as neurodegenerative diseases (e.g., Alzheimer's disease (AD) and amyotrophic lateral sclerosis) [6, 7], cerebrovascular diseases (e.g., stroke) [8], brain infections (e.g., meningitis) [9], and inflammatory disorders (e.g., multiple sclerosis) [10]. In addition to pathological conditions, many chemicals circulating in the blood could affect the BBB integrity [4]. Some of these chemicals are capable of increasing the BBB permeability while others have the opposite effect, i.e. improving tightness and function of the BBB [4].

In AD, BBB breakdown could range from mild disruption of TJs with enhanced BBB permeability to chronic integrity loss with altered transport of molecules across the BBB, brain hypo-perfusion and inflammatory responses [1]. Several studies have attributed these pathological changes in the BBB to accumulated amyloid-β peptides in the brain of AD patients. Increased levels of soluble Aβ have been shown to affect the BBB-endothelial cells integrity by reducing the expression and re-localization of TJ proteins [11]. In addition, reduction in transporters' expression and activity in the endothelial cells of human and rodents' BBB were observed when these cells were exposed to different amyloid preparations [12, 13].

To study the BBB biology and activity, several *in vivo*, *in vitro* and in silico models have been established [14–16]. *In-vivo* experiments provide the most reliable information on the BBB activity and integrity; however, the complexity of this model render its use for drug screening and urge the development of more feasible *in vitro* models for drugs screening [16, 17]. Nowadays, many *in vitro* models that are established from primary or immortalized ECs are available to study the BBB function [15, 18]. *In vitro* models assembled from primary ECs isolated from rodents' brains are usually preferred because they resemble the BBB endothelium characteristics; however, the yield of cell isolation and culturing is very low making this model inappropriate for high-throughput screening (HTS) purposes [16, 19, 20]. Other types of *in vitro* models utilize cells of epithelial origin such as MDCK cells; while these cells fulfill some BBB characteristics, they are not similar to the brain

Author Manuscript Author Manuscript Author Manuscript Author Manuscript

endothelium [21]. Thus, immortalized brain ECs are more beneficial over epithelial cells and mimic the BBB more closely [21, 22]. Immortalized brain ECs grown on a porous membrane coated with a substitute of basal lamina is the most widely used model to evaluate the BBB endothelium monolayer integrity [6, 15, 22]. In this model, ECs form a tight monolayer that could be easily manipulated by chemicals or a disease condition to study their effect on the barrier integrity of the ECs monolayer [23]. Although these models are currently available to investigate the dynamic function of the BBB in normal and pathological states [1, 14, 18, 24], none of them has been used for the screening of large number of compounds due to associated cost, reliability and time constraints [18, 23].

Accordingly, the first intent of this study was to upgrade and optimize a cell-based BBB model for HTS purposes. Following the model optimization to be suited for HTS, a large number of compounds were evaluated for their effect on the barrier integrity of the ECs-based BBB. Findings from the HTS identified two types of compounds; compounds that increase the BBB model permeability by disrupting TJs between ECs, and more vitally, compounds that enhance the TJs between ECs and decrease the BBB model permeability. In addition, among the identified integrity enhancers several FDA-approved drugs were recognized, a finding which is significant for their potential of repurposing to treat or prevent the BBB breakdown caused by amyloid-β in AD. Repurposing of FDA-approved drugs for the treatment of AD is an innovative approach because these drugs are well studies and evaluated, and thus could be taken forward to clinical trials.

Materials and Methods

Materials

Fibronectin from bovine plasma, Lucifer Yellow (LY) and compounds library LOPAC®1280 were purchased from Sigma-Aldrich (St. Louis, MO). HTS 3 μm polycarbonate membrane transwell 96-well plates and 0.45 μm polyester membrane transwell 24-well plates were purchased from Corning (Corning, NY). Rat-tail collagen type-I, sterile PBS, DMEM medium and penicillin/streptomycin antibiotics were obtained from Gibco (Grand Island, NY). ^{14}C-inulin ([carboxyl-^{14}C]-inulin, M.W.: 5000 Da) was purchased from American Radiolabeled Chemicals (St. Louis, MO). The MTT assay was obtained from Trevigen (Gaithersburg, MD). All other chemicals, reagents and supplies were purchased from VWR (West Chester, PA) and Sigma-Aldrich (St. Louis, MO).

Cell culture

The immortalized mouse brain endothelial cell line, bEnd3 was obtained from ATCC (Manassas, VA) and used as a representative model for the BBB endothelium [25, 26]. bEnd3 cells, passage 25–35, were cultured in DMEM supplemented with 10% fetal bovine serum (FBS), penicillin G (100 IU/ml), streptomycin (100 μg/ml), 1% w/v nonessential amino acids, and glutamine 2 mM. Cultures were maintained in a humidified atmosphere (5%CO_2/95% air) at 37°C and media was changed every other day. The human brain endothelial cell line hCMEC/D3 (kindly provided by Dr. P.O. Couraud, Institute Cochin, Paris, France), passage 25–30, were cultured in EBM-2 medium supplemented with 1 ng/ml human basic fibroblast growth factor (Sigma-Aldrich, MO), 10 mM HEPES, 1% chemically

Author Manuscript Author Manuscript Author Manuscript Author Manuscript

defined lipid concentrate (Gibco, NY), 5 μg/ml ascorbic acid, 1.4 μM hydrocortisone, 1% penicillin-streptomycin and 5% of heat-inactivated FBS "gold". Cultures were maintained in a humidified atmosphere (5%CO2/95% air) at 37°C.

Establishment of the BBB endothelium model for HTS

bEnd3 cells were plated onto HTS transwell 96-well plate with polycarbonate membrane inserts, 4.26 mm diameter with 3 μm pores size, at a seeding density of 50,000 cells/cm^2. To achieve optimal barrier integrity of bEnd3 cells, transwell membrane should be coated with basement membrane substitute (BM-substitute). Thus, we compared the barrier function of bEnd3 cells grown on transwells coated with different BM-substitutes including fibronectin from bovine plasma at concentrations of 30 and 60 μg/ml, rat-tail collagen type-I at concentrations of 150 and 300 μg/ml, or a mixture of fibronectin and collagen (30 and 150 μg/ml, respectively). For coating, 50 μl of BM-substitute diluted in sterile PBS was added to the apical side of each transwell filter. The transwell plate containing the filters was placed in a 37°C, 5% CO_2/95% air incubator for 2 h to form a coat. Before cells seeding, 150 μl fresh media were added to the apical side of each transwell filter, then the total volume of BM solution and media were removed by aspiration. For cell seeding, 50 μl of cell suspension were added to the apical side of each transwell filter and 200 μl of fresh media were added to the basolateral side. Cells were incubated at 37°C, 5% CO_2/95% air for 6 days. At the end of incubation period, barrier function of bEnd3 cells grown on the top of transwell filters coated with different types of BM-substitutes, transwell filters coated with different type of BM-substitutes (without cells), and transwell filters without coat were evaluated by measurement of LY permeation coefficient as described below.

Permeability assay

On the experiment day, the endothelial barrier integrity was evaluated by measuring LY permeation across immortalized mouse and human brain capillary endothelial cell lines. LY is a small, water-soluble molecule that travels across bEnd3 cells monolayer only through passive paracellular diffusion (i.e. through space between cells) [25], therefore, any changes in the tightness of bEnd3 monolayer will affect the permeation of LY. To initiate the transport experiment, 50 μl of transport buffer (141 mM NaCl, 4 mM KCl, 2.8 mM $CaCl_2$, 1 mM $MgSO_4$, 10 mM HEPES, and 10 mM D-glucose, pH 7.4) containing 100 μM LY was loaded onto the apical side of each transwell filter. Two hundred microliters of fresh and pre-warmed transport buffer were added to the basolateral side of each transwell filter. The transwell plate was then placed in a 37°C, 5% CO_2/95% air incubator for 1 h. LY concentrations in apical and basolateral compartments were determined by measuring their fluorescence intensities in addition to standards of LY of known concentrations at excitation and emission wavelengths of 485 and 529 nm, respectively (Synergy 2 microplate reader; Biotek, VT). Data acquisition was achieved using Gene5 software (Biotek, VT). Apparent permeation coefficient (Pc) was calculated from the following equation:

$$Pc\,(cm/sec) = \frac{V_b \times C_b}{C_a \times A \times T} \quad \text{Equation 1}$$

Author Manuscript Author Manuscript Author Manuscript Author Manuscript

where, V_b is the volume of basolateral side (200 μl), C_b is the concentration of LY (μM) in the basolateral side, C_a is the concentration of LY (μM) in the apical side, A is the membrane area (0.143 cm^2), and T is the time of transport (3600 sec). In addition, permeability measurements from 1 to 7 days of seeding were analyzed to determine the day on which bEnd3 cells forms the tightest monolayer measured as lowest LY permeation (i.e. day of maximum barrier integrity).

bEnd3 cells growth assay

To monitor the growth of bEnd3 cells on the top of coated transwell membrane, number of viable cells was daily assessed using the MTT assay. MTT assay is based on the reduction of a highly water-soluble tetrazolium dye by mitochondrial dehydrogenase to insoluble purple formazan. MTT assays were performed daily starting on day 1 to day 7 of seeding as described previously [27]. Trans-epithelial electrical resistance (TEER) was also performed and measured using an EVOM epithelial volt-ohmmeter with STX2 electrodes (World Precision Instruments, FL).

Model and assay validation

To validate the barrier function of the optimized bEnd3 monolayer, we compared LY permeation across bEnd3 monolayer grown on top of 3 μm polycarbonate membrane to cells grown on top of 0.45 μm polyester membrane. Both membranes were coated with 30 μg/ml fibronectin, seeded with 1750 cells per well (seeding density of 50,000 cells/cm^2), and allowed to grow for 6 days for tight monolayer formation. LY permeation assay was performed on day 6 as described above. Moreover, we validated LY as a marker for paracellular diffusion by comparing its permeation across bEnd3 monolayer to the permeation of ^{14}C-inulin ([carboxyl-^{14}C]-inulin, M.W.: 5000 Da). Inulin is a large molecule that has been used as a paracellular permeability marker [28]. For inulin permeation, 50 μl of transport buffer containing 0.05 mM ^{14}C-inulin was added to the apical chamber, and 200 μl of pre-warmed transport buffer was added to the basolateral chamber. Cells were maintained in a humidified atmosphere (5%CO_2/95% air) at 37°C for 1 h. Fifty microliter aliquots from the apical and basolateral chambers were collected at the end of incubation period. After mixing samples with 1 ml of scintillation cocktail, ^{14}C-inulin dpm was measured using a Wallac 1414 WinSpectral Liquid Scintillation Counter (PerkinElmer, MA). Concentrations of ^{14}C-inulin in apical and basolateral side were calculated in dpm/ml. The Pc of ^{14}C-inulin (cm/sec) was calculated using equation 1 as described above.

Quality control of the model

To investigate robustness and performance of the optimized bEnd3 monolayer as a BBB model for HTS, the Z′ factor, signal-to-noise ratios (S/N), and signal-to-background ratios (S/B) were calculated for 30 randomly selected plates performed on ten different days. DMSO (0.1%) was used as negative control, 1.4 M mannitol, and 10 μM hydrocortisone were used as positive controls to evaluate the performance of bEnd3 monolayer in HTS. The Z′-factor, S/N, and S/B were considered as criteria for data quality and were calculated according to the following equations [29]:

Author Manuscript Author Manuscript Author Manuscript Author Manuscript

$$Z'factor = 1 - \frac{3 * \text{SD Hydrocortisone or Mannitol} + 3 * \text{SD DMSO control}}{|\text{Mean Hydrocortisone or Mannitol} - \text{Mean DMSO control}|} \quad \text{Equation 2}$$

$$S/N = \frac{|\text{Mean Hydrocortisone or Mannitol} - \text{Mean DMSO control}|}{\text{SD DMSO control}} \quad \text{Equation 3}$$

$$S/B = \frac{\text{Mean Hydrocortisone or Mannitol}}{\text{Mean DMSO control}} \quad \text{Equation 4}$$

Where SD is standard deviation.

Compounds screening

Sigma LOPAC®1280 library, containing 1280 pharmacologically active compounds with known mechanisms, was used for compounds screening. These compounds were screened for their effects on the barrier integrity of bEnd3 monolayer using the LY permeation assay described above. Compounds were added to the apical side of the transwells on day 5 of seeding after dilution in DMEM to a final concentration of 10 μM. This dilution resulted in a final 0.1% DMSO concentration. Preliminary studies showed that this DMSO concentration has no effect on the integrity of bEnd3 monolayer, and were included as a negative control. The concentration 10 μM was selected for screening based on available studies [30, 31]. Each compound was tested in 6 replicates. Plates were incubated with drugs for 24 h at 37°C, 5% CO_2/95% air. At the end of treatment period (day 6 post-seeding), LY permeation assay was performed and the Pc was calculated as described above. For each compound, the average Pc of the 6 replicate was normalized to a *z*-score based on the median and MAD (median absolute deviation) values of each plate. The *z*-score was calculated from the following equation [32]:

$$z - score = \frac{\text{x} - \text{Óij}}{\text{MAD}} \quad \text{Equation 5}$$

where x is the mean of the Pc after treatment with each compound, X̧ is the median across all compounds in the plate without controls, and MAD is median absolute deviation across all compounds in the plate [MAD = 1.4826 × X̧ × (|x − X̧ |)]. A compound with *z*-score > 3 (i.e. increased permeability by more than 3 MADs) was considered a “disruptor” to bEnd3 monolayer integrity as it significantly increased LY permeation, while a compound with *z*-score < −2 (i.e. reduced permeability by more than 2 MADs) was considered as “enhancer” or a “hit” and was further selected for secondary concentration-dependent screening. Hits that are FDA approved drugs and demonstrated reduced Pc were selected for secondary confirmatory screening. In the secondary screen, hits were first tested in a 6-point concentration-response series (0.75–10 μM) using the LY permeation assay, then confirmed

Author Manuscript Author Manuscript Author Manuscript Author Manuscript

hits were re-tested in a 10-point concentration-response studies ranging from 0.065 to 20 μM to calculate the EC_{50} value for each compound. All Curve fittings were performed using GraphPad Prism (Version5, GraphPad Software, CA) software.

Western blot analyses of tight junction protein claudin-5

bEnd3 cells (50,000 cells/cm^2) were seeded in 10 mm dishes for western blot analysis and allowed to grow to 70% confluency before treatment with drugs in a humidified atmosphere (5%CO_2/95% air) at 37°C. On day 5 post-seeding, cells were treated with 10 μM of control and hit compounds for 24 h. At the end of treatment period, cells were lysed with RIPA buffer containing complete mammalian protease inhibitors. 25 μg of cellular protein was resolved on 8% Bis-tris gels and electrotransferred onto 0.45 μm nitrocellulose membrane. Membranes were blocked with 2% BSA and incubated overnight with monoclonal antibody for claudin-5 (H-52; Santa Cruz) or actin (Santa Cruz) at dilutions 1:200. For antigen detection, HRP-labeled secondary IgG antibody for claudin-5 (anti-rabbit) and actin (anti-rabbit) (Santa Cruz) at 1:2000 dilutions were used. The bands were visualized using a SuperSignal West Femto detection kit (Thermo Scientific, IL). Quantitative analysis of the immunoreactive bands was performed using Li-Core luminescent image analyzer (LI-COR Biotechnology, NE) and band intensity was measured by densitometric analysis. Three independent Western blotting experiments were carried out for each treatment group.

Immunostaining of the tight junction claudin-5

On day 6, cells treated on previous day with hit compounds were pre-fixed with 1:1 ratio of ice cold PBS and 4% formaldehyde for 5 min, followed by washing. Cells were then fixed with 4% formaldehyde/PBS for 10 min, permeabilized with 0.2%TritonX-100 for 10 min, blocked for 1 h then washed with PBS. Claudin-5 was visualized using the mouse monoclonal antibody claudin-5-Alexa Fluor 488 (Thermo Scientific) added to the cells and kept overnight at 4 °C; nuclear staining was performed with 4′,6-diamidino-2-phenylindole for 10 min. Cells were observed using Nikon Eclipse Ti-S inverted fluorescence microscope (Norcross, GA) at a total magnification of 20X.

Effect of hit FDA compounds on compromised bEnd3 cells-based BBB model by amyloid-β

Solutions of synthetic amyloid-β (Aβ) peptides including $A\beta_{40}$, $A\beta_{42}$ and $A\beta_{42}$ oligomers were prepared and characterized as described previously [33]. Aβ mixtures were prepared by mixing $A\beta_{40}$ monomers (100 nM) and $A\beta_{42}$ oligomers (200 nM). On day 5 of seeding, Aβ mixture was added to the basolateral side of the transwells and hit compounds were added to the apical side (each at 10 μM). Twenty four hours later the LY permeation assay was performed as described above to monitor the ability of hit compounds to rectify the BBB model tightness compromised by Aβ mixture.

Effect of hit FDA compounds on rectifying the disruptive effect of Aβ mixture in hCMEC/D3 cells-based BBB model

The translational potential of findings from the mouse endothelial cells bEnd3 was tested using the human brain endothelial cell line hCMEC/D3. hCMEC/D3 were grown on inserts to form a monolayer as described previously by us [33–35]. On day 5, cells were treated for

Author Manuscript Author Manuscript Author Manuscript Author Manuscript

24 h with control media or mixture of 100 nM monomeric $A\beta_{40}$ and 50 nM $A\beta_{42}$ oligomers added to the basolateral side of the transwells and hit compounds added to the apical side (each at 10 μM) as described previously [33]. On the next day, LY permeation assay was performed as described above to monitor the ability of compounds to rectify cells monolayer tightness compromised by Aβ mixture.

Statistical analysis

Unless otherwise indicated, the data were expressed as mean ± SEM. The experimental results were statistically analyzed for significant difference using two-tailed Student's t-test for two groups, and one-way analysis of variance (ANOVA) for more than two groups' analysis. Values of $P<0.05$ were considered statistically significant.

Results

A schematic presentation of the model and its application is demonstrated in Scheme 1.

Coating optimization

For optimal growth and to form a tight monolayer that could simulate the BBB endothelial function, bEnd3 cells should be grown on the top of supporting membrane coated with a BM-substitute. Thus, to find a suitable BM-substitute that offers high restriction for paracellular diffusion in the presence of a cell monolayer while providing weak barrier properties in the absence of cells, we have screened 2 types of BM-substitutes. Fibronectin and rat-tail collagen type I were investigated as both are commonly used BM-substitutes that support the growth of bEnd3 cells [36, 37]. In the absence of cells, collagen (300 μg/ml), fibronectin (60 μg/ml), and a mixture of collagen (150 μg/ml) and fibronectin (30 μg/ml) formed a barrier to LY permeation, which is based on the measurement of LY Pc as a paracellular diffusion marker (Figure 1a) [26]. On the other hand, LY permeation across wells coated with collagen (150 μg/ml) or fibronectin (30 μg/ml) showed comparable LY permeation to that of uncoated wells indicative that both coatings did not form a barrier restricting LY permeation (Figure 1a). In the presence of cells, among both, fibronectin at 30 μg/ml significantly reduced the Pc of LY (Pc = $3.5\times10^{-5} \pm 2.7\times10^{-6}$ cm/sec; $P<0.001$) compared to collagen at 150 μg/ml (Pc of $7.9\times10^{-5} \pm 1.8\times10^{-6}$ cm/sec) (Figure 1a). Based on these results, 30 μg/ml fibronectin for coating was selected and used in all subsequent experiments.

Permeability, resistance and growth assessment of bEnd3 monolayer

For selection of the optimal day for compounds treatment and permeability screening, we daily monitored the growth of bEnd3 cells and LY permeation up to 7 days post-seeding. Figure 1b shows a linear increase in the number of cells from day 1 to 3 post-seeding (doubling time is 24 h), reaching a plateau on days 3–6 where cells number did not significantly increase indicating the formation of confluent monolayer. Consistent with the cells growth pattern, the monolayer was leaky on day 1 as demonstrated by the LY permeation coefficient values (Figure 1b), which gradually decreased with time up to day 4 demonstrating the formation of a tight monolayer. LY permeation coefficient remained almost constant between days 4–6 post-seeding (Pc ~ 4.0×10^{-5} cm/sec) indicative of tight

Author Manuscript Author Manuscript Author Manuscript Author Manuscript

junction formation restricting the paracellular permeation of LY (Figure 1b). On day 7, the reduction in cells number was correlated with the increase in LY permeation indicating initiation of cells de-attachment or death. According to these results, all consequent studies were performed on day 5 for compounds treatment for 24 h followed by LY permeation assay on day 6. In addition and consistent with cells growth and LY permeation behavior, the monolayer resistance monitored by TEER measurements demonstrated a TEER value of ~35Ω.cm^2 on days 5 and 6 post-seeding, which is consistent with our previous studies observed with intact monolayer [33–35].

Model validation

To validate the barrier function of the *in vitro* BBB model, LY permeation across bEnd3 monolayer grown on top of 3 μm polycarbonate or 0.45 μm polyester transwell inserts were compared. Polyester membrane with 0.45 μm pore size is a well-established supporting membrane that has been used by many investigators to establish tight endothelial cells monolayer for drug permeability studies [22, 38]; however, this type of membrane is costly for HTS. Our results showed comparable LY Pc values between the two membrane types (Figure 2a). Moreover, we optimized the use of LY as a marker for paracellular permeability by comparing its permeation coefficient to that of inulin. Our result showed that inulin has significantly lower permeation coefficient than LY (Pc = $3.8\times10^{-6} \pm 4.3\times10^{-7}$ vs $3.5\times10^{-5} \pm 1.5\times10^{-6}$ cm/sec, respectively; Figure 2b). However, both paracellular permeation markers showed similar pattern in the absence or presence of bEnd3 monolayer, therefore, LY was selected as a paracellular marker for subsequent studies due to its feasibility and practicality over the use of radioactive inulin.

Quality control of established model for HTS

To evaluate the model performance for HTS of compounds, Z′ factor, signal-to-noise (S/N) and signal-to-background (S/B) ratios were calculated from 30 representative plates (Figure 3). The Z′ factor serves as an indicator of assay quality and takes into account the variability in samples data [29]. For cell-based assays, a Z′ value of 0.5 is an acceptable measure with favorable assay quality. The S/N and S/B are measures for the ability of the system to differentiate between positive and negative controls [29]. In this study, we used this model to identify two types of compounds: compounds that increase LY permeation by disrupting the integrity of bEnd3 monolayer, and compounds that decrease LY permeation by enhancing bEnd3 monolayer integrity. To evaluate the model performance and its ability to identify compounds that increase LY permeation, mannitol (1.4 M) was used as a positive control for compounds that disrupt the integrity of bEnd3 monolayer [39]. The model demonstrated excellent performance to identify disruptors with a Z′ factor above 0.5 and high S/N and S/B ratios across 30 independent plates (Figure 3). On the other hand, hydrocortisone (10 μM) was used as a positive control for compounds that enhance integrity and barrier function of bEnd3 monolayer, as it is known to improve tightness of endothelial monolayer by enhancing the expression of TJs proteins [40, 41]. The Z′ factor determined with hydrocortisone was 0.3 ± 0.11 with lower S/N and S/B ratios compared to those with mannitol (Figure 3).

Author Manuscript Author Manuscript Author Manuscript Author Manuscript

Screening of LOPAC®1280 library

The model was then used to screen Sigma LOPAC®1280 library comprising of 1280 compounds for enhancers of the *in vitro* BBB endothelium model tightness. All compounds were tested at concentration of 10 μM in 6 replicates. The apparent Pc was converted to *z*-score for each screened compound (Figure 3). In each plate, normalized LY Pc for most compounds followed a normal distribution centered on the plate median. Using the cut-off criteria for disruptors and enhancers, we could identify 62 compounds as disruptors with *z*-score greater than 3 MADs from plate median, and 50 compounds as enhancers with *z*-score less than −2. Out of the 50 compounds that were able to enhance bEnd3 monolayer integrity, there were 10 FDA approved drugs that are in clinical use. In order to assess repurposing opportunities, the effect of these FDA approved drugs on the monolayer integrity was further tested by performing a 6-point concentration-response studies, from which 7 drugs were emerged as hits, while the remaining drugs were excluded from further screening due to their lack of concentration-dependent change in LY permeation (Supplementary figure 1). The selected 7 hits were then validated in 10-point concentration-response studies in the range 0.065–20 μM to calculate their EC_{50} (Table 1). As these tested drugs were toxic to the cells at the concentration 20 μM, the EC_{50} was estimated from the concentration range 0.065–15 μM. The 7 drugs showed a sigmoidal concentration-response reduction in LY permeation across the bEnd3 monolayer with EC_{50} values ranging from 0.76–4.56 μM (Figure 4 & Table 1). On the other hand, the primary screen has identified 62 compounds that increased LY permeation across bEnd3 monolayer indicating a disruption in its integrity. Table 2 shows 10 FDA approved drugs that were identified as disruptors when tested at 10 μM concentration.

Effect of hit FDA-approved drugs on claudin-5 expression

Hit FDA drugs were further investigated for potential mechanisms by which these drugs enhanced the BBB model integrity. For this, expression of the tight junction protein claudin-5 was evaluated by immunocytochemistry and Western blot. Claudin-5 was specifically evaluated as previous studies have shown hydrocortisone (the positive control used in the current study) to enhance BBB tightness via up-regulation of claudin-5 expression [40, 41]. The expression and localization of claudin-5 in bEnd3 monolayer using immunocytochemistry analysis demonstrated oxaprozin, etodolac, beclomethasone and candesartan to significantly induce claudin-5 expression ($p<0.05$, Figure 5a). Similarly, Western blot analysis showed tested compounds to increase claudin-5 expression by 15–40% with the highest and significant increase observed with the drugs oxaprozin, etodolac and beclomethasone when compared to DMSO treated cells ($p<0.05$, Figure 5b).

Protective effect of hit FDA drugs against amyloid vascular toxicity in bEnd3 cells

We evaluated the potential of the hit FDA drugs to improve and rectify the disruptive effect of Aβ mixture. This study was performed based on our previous report [33]. As shown in Figure 6a, the addition of Aβ mixture (100 nM $A\beta_{40}$ monomers and 200 nM $A\beta_{42}$ oligomers) to the basolateral side for 24 h caused a significant increase in LY permeation by 45% compared to control treated cells ($p<0.05$). Simultaneous treatment with the hit FDA drugs demonstrated that all drugs, except tomoxetine and pancuronium, to rectify the

Author Manuscript Author Manuscript Author Manuscript Author Manuscript

disruptive effect of Aβ mixture to levels comparable to those of control ($p<0.05$, Figure 6a). Pancuronium showed a trend toward reduction, however the effect was not statistically significant from that of Aβ mixture only treated cells ($p>0.05$).

Hit FDA drugs have deferential effect against amyloid vascular toxicity in hCMEC/D3 cells

To evaluate whether the protective effect of hit FDA drugs observed in bEnd3 could be extended to humans, these drugs were tested for their potential to rectify the toxic effect of Aβ mixture (50 nM $A\beta_{40}$ monomers and 100 nM $A\beta_{42}$ oligomers) in hCMEC/D3. As shown in Figure 6b, 24 h treatment with the hit FDA drugs demonstrated that only etodolac, granisetron and beclomethasone to significantly reduce the disruptive effect of Aβ mixture on the BBB model integrity.

Discussion

Brain capillaries are characterized by forming the BBB that maintains constant brain homeostasis and protects the brain from free entry of different substances that could interrupt with normal neural activity [5, 42]. Brain ECs, BM, neurons, astrocytes and pericytes play important role in supporting the normal function of the BBB [4]. Both pericytes, the uniquely positioned cells within the neurovascular unit, and astrocytes, the most abundant glial cells in the brain, significantly contribute to the unique properties of the ECs in forming a tight BBB [43]. Recent studies have suggested the malfunction of pericytes and astrocytes in AD that contribute to the vascular pathology associated with AD [44, 45]. The reason(s) of pericytes loss in AD is not completely understood, and it is yet to be determined whether their degeneration observed in AD is a consequence of risk factors such as stroke [46], diabetes [47] and brain injury [48], or is Aβ-mediated. Several studies have suggested that Aβ accumulation in pericytes could overwhelm its own clearance and cause pericytes degeneration [49, 50]. Besides, reactive astrocytes have been also observed in chronic neurodegenerative lesions and contribute to neuronal as well as vascular pathogenesis in AD [45]. However, while astrocytes, pericytes and BM play important role in regulating and supporting the BBB integrity and function, only the capillary endothelium forms the physical barrier separating brain from blood [23]. Therefore, in this study, an *in vitro* ECs-based BBB model was used, first, because ECs are the main cellular component of the BBB that confer the barrier function [42], and second for practicality reasons that allow HTS of large number of compounds.

In this study, a cell-based assay that effectively represents the barrier function of the BBB endothelium was optimized to screen a library of compounds for their effects on the BBB endothelium integrity. This model was able to identify 2 set of compounds; compounds that disrupt the BBB endothelium integrity, which might contribute to the development of neurological diseases, and compounds that enhance the BBB integrity and thus could be helpful in the treatment of many neurological diseases including AD and cerebral amyloid angiopathy (CAA).

bEnd3 cell line was used to develop the BBB model that is appropriate for HTS because it possesses several features over primary ECs including simple seeding and rapid formation of tight monolayer, characteristics that makes it suitable for sensitive and compatible HTS

Author Manuscript Author Manuscript Author Manuscript Author Manuscript

assay. Besides, bEnd3 cells express most of the properties of *in vivo* brain ECs such as the expression of TJ proteins, transport proteins and receptors, in addition to their ability to form a tight polarized monolayer restricting the paracellular permeability [20, 51]. While several *in-vitro* BBB models have been recently developed, none of these models was upgraded for HTS [14–16]. Therefore, the key objectives of this work were first to increase the capacity of available *in vitro* BBB models for HTS assays, and second to screen large number of compounds for their effect on integrity of the *in vitro* BBB model.

Before using the bEnd3 cells-based BBB model for compounds screening, the model was optimized and validated with a series of experiments that aimed to attain maximal barrier integrity for bEnd3 monolayer. Consistent with previous studies, we found that polycarbonate membrane with pore size of 3 μm coated with 30 μg/ml fibronectin as a BM-substituent was optimal to enhance the growth of bEnd3 cells and produce a tight monolayer [20, 22, 25, 26, 52]. This combination of the cell-based system and the use of 96-well polycarbonate membrane guaranteed low cost, with high sensitivity and HTS capability.

To test the performance of the optimized bEnd3 monolayer, the Z′ factor, S/N and S/B were calculated as measures for the HTS performance of the model [29]. The model performance was evaluated using two positive controls, mannitol as a positive control for compounds disruptors [39], and hydrocortisone for integrity enhancers [40, 41]. While the assay demonstrated an excellent performance to identify disruptors, the assay exhibited a smaller separation, but significant, between the negative control and hydrocortisone treatment (Z′ factors = 0.3 ± 0.11). A Z′ factor of 0.3 is considered an acceptable value for this HTS performance because hydrocortisone enhanced the barrier function of the already tight monolayer, hence, LY permeation is not expected to largely deviate from the negative control treatment like that observed with disruptors. Hydrocortisone's enhancement of the barrier function caused 25% reduction in LY permeation coefficient. Moreover, a Z′ factor of less than 0.5 has been reported with HTS assays that screen for agonists because it depends on the potency of the positive control in use [53]. To increase the confidence of hits selection, we tested each compound in 6 replicates. Increasing number of replicates enhances the assay performance by decreasing the imprecision of the assay (standard error) [54]. The use of 6 replicates for each compound decreased the imprecision of our assay by ~63% making this optimized bEnd3 monolayer a powerful tool for hits identification [54]. In further support for the validity of the assay and selection criteria, from the primary screen, among the compounds that have been identified as BBB integrity enhancers was the positive control hydrocortisone, which was blindly tested as part of the library; and among the disruptors was ammonia which is known to have a toxic effect on the BBB [55].

Using the aforementioned optimized model and hit selection analysis, we carried out an initial screen of Sigma LOPAC®1280 library compounds for their effect on the integrity of bEnd3 monolayer. For hits selection, we used a more sophisticated approach to improve overall confirmation rates that is based on median and median absolute deviation (MAD) of the plate instead of mean and standard deviation [32]. Median and MAD values are resistant to the presence of outliers, and hits selection by the MAD-based method include all the hits that would be selected by the SD-based method with a significant number of additional hits [32]. The results of this screen identified 62 compounds that disrupted the barrier integrity of

Author Manuscript Author Manuscript Author Manuscript Author Manuscript

bEnd3 monolayer, and 50 compounds that enhanced the monolayer integrity. In the current study, the only therapeutic or clinical envision from identification of compounds that disrupt bEnd3 monolayer integrity is to show possible adverse effect of these compounds if they are FDA approved drugs. On the other hand, identifying compounds that enhance the barrier function of the bEnd3 monolayer could have a broad spectrum of clinical applications in treatment or prevention of BBB breakdown associated with different neurological diseases such as AD and CAA [4, 15, 23]. Among the 50 compounds that enhanced the bEnd3 monolayer integrity 10 hits were FDA approved drugs. Seven of hhese hit FDA drugs were further selected for the secondary screening and EC_{50}s calculation. Then, these drugs were tested for their protective effect against Aβ toxicity. Previous reports suggested repurposing of FDA approved drugs as an efficient drug discovery strategy to identify drugs that could be used in the treatment of neurological diseases including AD [56–58]. This strategy offers an alternative and cost-effective drug development approach with potential to identify new treatments in a fraction of the time required to develop a treatment from scratch [56].

Available evidences from biochemical, genetic and animal studies implicate Aβ as a pathogenic peptide in AD [59]. The amyloid cascade hypothesis stated that AD is caused by an imbalance between Aβ production and clearance, resulting in an increased amount of Aβ in various forms such as monomers, oligomers, insoluble fibrils, and plaques in the CNS. In AD, clearance of Aβ from the brain takes place by three pathways; (a) transport across the BBB [7], (b) degradation in the brain tissue which is mediated by specific Aβ degrading enzymes or by glial cells uptake and lysosomal degradation [60]; and (c) the bulk flow of the ISF into the cerebrospinal fluid (CSF) [61]. Among the 3 pathways, Aβ transport across the BBB has the highest contribution to the overall brain clearance with estimated clearance of 62% in mice [35]. As a peptide, Aβ has a poor passive membrane permeability and it depends on a transport system to cross the endothelial cells of the BBB [62]. This transport system consists of multiple receptors and transport proteins at the BBB such as the low-density lipoprotein receptor-related protein-1 (LRP1) and P-glycoprotein (P-gp) [63, 64]. In AD, both transport proteins are downregulated and contribute to Aβ cerebral accumulation [13, 33]. While multiple pathological alterations in AD brains could contribute to vascular dysfunction [53, 65–67], findings from AD patients' brains and preclinical studies using AD mice models also support the disruptive effect of increased brain levels of Aβ on the integrity and function of the BBB [11, 68–70]. This breakdown in the BBB integrity was associated with uncontrolled molecular transport and solute exchange [71], and reduced expression and re-localization of TJ proteins [11, 65, 69, 70]. Accordingly, such alterations in the BBB observed in AD point toward the BBB as a target for therapeutic interventions to improve or rectify the BBB normal activity [34, 72]. In search for such therapeutics, our HTS identified 7 FDA approved drugs that enhanced bEnd3 monolayer integrity and demonstrated a sigmoidal concentration-response curve with low EC_{50}. These drugs were then evaluated for their potential to rectify the BBB breakdown caused by Aβ, similar to that observed in AD. When tested in the bEnd3 cells-based BBB model, the FDA drugs granisetron, candesartan, beclomethasone, etodolac and oxaprozin demonstrated a significant potential to ameliorate the integrity of the BBB model exposed to Aβ mixture of oligomers and monomers. Interestingly, however, when these hits tested for their translational potential to humans in hCMEC/D3-based BBB model, only etodolac,

Author Manuscript Author Manuscript Author Manuscript Author Manuscript

granisetron and beclomethasone demonstrated a significant reduction in LY permeation when compared to Aβ mixture treated cells ($p<0.05$), suggesting that these drugs were able to rectify the toxic effect of Aβ. Collectively, the above findings propose species differences; while 5 out of the 7 drugs demonstrated a positive effect in bEnd3 cells-based BBB model, only 3 drugs were able to rectify the disruptive effect of Aβ mixture in hCMEC/D3-BBB model. This difference, however, is not surprising. In a recent study, we reported differences between bEnd3 and hCMEC/D3 cells where the former cell line is metabolically more active than the latter and clear Aβ species (by degradation) at higher rate [35], which is also supported by *in vivo* findings. Besides, granisetron and etodolac belong to drug classes that have demonstrated beneficial effects against AD [74–81]. Members of the 5-HT3 receptor antagonists, like granisetron, have shown beneficial effect on memory and learning where it prevented age-induced memory loss in mice [74], and attenuated Aβ-induced neurotoxicity in cultured rat cortical neurons [75]. Similarly, when administered to scopolamine-induced memory-impaired mice, granisetron improved spatial recognition memory and fear memory [76]. The NSAID drug etodoloc, on the other hand, while studies evaluating its specific effect in AD are not available, studies examined other members of NSAIDs drugs exist. The beneficial effect of NSAIDs in AD remains controversial; however, several epidemiological studies reported the long-term use of NSAIDs is inversely associated with AD that may be modified by APOE genotype [77–79]. These results were supported by preclinical studies in transgenic mouse models of AD. For example, when tested in 3×Tg-AD [80] and Tg2576 mice [81] ibuprofen reduced Aβ plaques load and $A\beta_{42}$ levels. But when evaluated for their therapeutic effect against AD in clinical studies, NSAIDs treatment failed to enhance the cognitive function in AD patients [82–84]. Further studies are required to explain such inconsistencies and to confirm the effect of NSAIDs in AD. Nonetheless, findings of current study suggest positive effect of etodolac against Aβ toxic effect on the BBB *in vitro* model integrity, an effect that was not previously reported with other NSAIDs members. For the efficient translation of the current findings, the 2 drugs, granisetron and etodolac, which demonstrated ability to ameliorate and/or protect the mouse and human ECs-based BBB models will be further evaluated *in vivo* in AD mouse models.

In conclusion, this study offers for the first time, a cell-based assay that effectively represents the barrier function of the BBB endothelium for high-throughput screening of compounds for their effects on the barrier integrity. Moreover, we were able to identify FDA approved drugs that could enhance and rectify the integrity of endothelial monolayer and protect from amyloid toxicity in both mouse and human derived endothelial cell lines. These drugs, mainly etodolac, granisetron and beclomethasone, could be further *in vivo* evaluated for their ability to rectify the BBB function and treatment of many neurological diseases including AD. Finally, results of the current study suggest that pharmacological targeting of the BBB to enhance its function and integrity could potentially help treat and/or hold the progression of Aβ related disorders AD and CAA.

Supplementary Material

Refer to Web version on PubMed Central for supplementary material.

Author Manuscript Author Manuscript Author Manuscript Author Manuscript

Acknowledgments

This research work was funded by an Institutional Development Award (IDeA) from the National Institute of General Medical Sciences of the National Institutes of Health under grant number P20GM103424, by Louisiana Board of Reagent's Research Competitive Program under grant number LEQSF(2013–16)-RD-A-16, and by National Institute of Neurological Disorders and Stroke under grant number R15NS091934.

Abbreviations

BBB	blood-brain barrier
bEnd3	mouse brain endothelial cells
BM	basement membrane
EC	endothelial cells
HTS	High-throughput screening
LY	Lucifer Yellow
MAD	median absolute deviation
Pc	permeation coefficient
S/N	signal-to-noise
S/B	signal-to-background
TJ	tight junction
AJ	adherens junction.

References

1. Zlokovic BV. The blood-brain barrier in health and chronic neurodegenerative disorders. Neuron. 2008; 57:178–201. [PubMed: 18215617]
2. Banks WA. Characteristics of compounds that cross the blood-brain barrier. BMC Neurol. 2009; 9(Suppl 1):S3. [PubMed: 19534732]
3. Hawkins BT, Davis TP. The blood-brain barrier/neurovascular unit in health and disease. Pharmacol Rev. 2005; 57:173–185. [PubMed: 15914466]
4. Abbott NJ, Ronnback L, Hansson E. Astrocyte-endothelial interactions at the blood-brain barrier. Nat Rev Neurosci. 2006; 7:41–53. [PubMed: 16371949]
5. Rosenberg GA. Neurological diseases in relation to the blood-brain barrier. J Cereb Blood Flow Metab. 2012; 32:1139–1151. [PubMed: 22252235]
6. Zhong Z, Deane R, Ali Z, Parisi M, Shapovalov Y, O'Banion MK, Stojanovic K, Sagare A, Boillee S, Cleveland DW, Zlokovic BV. ALS-causing SOD1 mutants generate vascular changes prior to motor neuron degeneration. Nat Neurosci. 2008; 11:420–422. [PubMed: 18344992]
7. Bell RD, Zlokovic BV. Neurovascular mechanisms and blood-brain barrier disorder in Alzheimer's disease. Acta Neuropathol. 2009; 118:103–113. [PubMed: 19319544]
8. Yang Y, Estrada EY, Thompson JF, Liu W, Rosenberg GA. Matrix metalloproteinase-mediated disruption of tight junction proteins in cerebral vessels is reversed by synthetic matrix metalloproteinase inhibitor in focal ischemia in rat. J Cereb Blood Flow Metab. 2007; 27:697–709. [PubMed: 16850029]

Author Manuscript Author Manuscript Author Manuscript Author Manuscript

9. Leppert D, Lindberg RL, Kappos L, Leib SL. Matrix metalloproteinases: multifunctional effectors of inflammation in multiple sclerosis and bacterial meningitis. Brain Res Brain Res Rev. 2001; 36:249–257. [PubMed: 11690622]
10. Henderson AP, Barnett MH, Parratt JD, Prineas JW. Multiple sclerosis: distribution of inflammatory cells in newly forming lesions. Ann Neurol. 2009; 66:739–753. [PubMed: 20035511]
11. Gonzalez-Velasquez FJ, Kotarek JA, Moss MA. Soluble aggregates of the amyloid-beta protein selectively stimulate permeability in human brain microvascular endothelial monolayers. J Neurochem. 2008; 107:466–477. [PubMed: 18702666]
12. Qosa H, Abuznait AH, Hill RA, Kaddoumi A. Enhanced brain amyloid-beta clearance by rifampicin and caffeine as a possible protective mechanism against Alzheimer's disease. J Alzheimers Dis. 2012; 31:151–165. [PubMed: 22504320]
13. Brenn A, Grube M, Peters M, Fischer A, Jedlitschky G, Kroemer HK, Warzok RW, Vogelgesang S. Beta-Amyloid Downregulates MDR1-P-Glycoprotein (Abcb1) Expression at the Blood-Brain Barrier in Mice. Int J Alzheimers Dis. 2011; 2011:690121. [PubMed: 21660212]
14. Abbott NJ, Dolman DE, Patabendige AK. Assays to predict drug permeation across the blood-brain barrier, and distribution to brain. Curr Drug Metab. 2008; 9:901–910. [PubMed: 18991587]
15. Wong AD, Ye M, Levy AF, Rothstein JD, Bergles DE, Searson PC. The blood-brain barrier: an engineering perspective. Front Neuroeng. 2013; 6:7. [PubMed: 24009582]
16. Geldenhuys WJ, Allen DD, Bloomquist JR. Novel models for assessing blood-brain barrier drug permeation. Expert Opin Drug Metab Toxicol. 2012; 8:647–653. [PubMed: 22468700]
17. Deguchi Y, Morimoto K. Application of an in vivo brain microdialysis technique to studies of drug transport across the blood-brain barrier. Curr Drug Metab. 2001; 2:411–423. [PubMed: 11766991]
18. Wilhelm I, Fazakas C, Krizbai IA. In vitro models of the blood-brain barrier. Acta Neurobiol Exp (Wars). 2011; 71:113–128. [PubMed: 21499332]
19. Steiner O, Coisne C, Engelhardt B, Lyck R. Comparison of immortalized bEnd5 and primary mouse brain microvascular endothelial cells as in vitro blood-brain barrier models for the study of T cell extravasation. J Cereb Blood Flow Metab. 2011; 31:315–327. [PubMed: 20606687]
20. Brown RC, Morris AP, O'Neil RG. Tight junction protein expression and barrier properties of immortalized mouse brain microvessel endothelial cells. Brain Res. 2007; 1130:17–30. [PubMed: 17169347]
21. Hellinger E, Veszelka S, Toth AE, Walter F, Kittel A, Bakk ML, Tihanyi K, Hada V, Nakagawa S, Duy TD, Niwa M, Deli MA, Vastag M. Comparison of brain capillary endothelial cell-based and epithelial (MDCK-MDR1, Caco-2, and VB-Caco-2) cell-based surrogate blood-brain barrier penetration models. Eur J Pharm Biopharm. 2012; 82:340–351. [PubMed: 22906709]
22. Weksler BB, Subileau EA, Perriere N, Charneau P, Holloway K, Leveque M, Tricoire-Leignel H, Nicotra A, Bourdoulous S, Turowski P, Male DK, Roux F, Greenwood J, Romero IA, Couraud PO. Blood-brain barrier-specific properties of a human adult brain endothelial cell line. FASEB J. 2005; 19:1872–1874. [PubMed: 16141364]
23. Cecchelli R, Berezowski V, Lundquist S, Culot M, Renftel M, Dehouck MP, Fenart L. Modelling of the blood-brain barrier in drug discovery and development. Nat Rev Drug Discov. 2007; 6:650–661. [PubMed: 17667956]
24. Zehendner CM, Librizzi L, de Curtis M, Kuhlmann CR, Luhmann HJ. Caspase-3 contributes to ZO-1 and Cl-5 tight-junction disruption in rapid anoxic neurovascular unit damage. PLoS One. 2011; 6:e16760. [PubMed: 21364989]
25. Omidi Y, Campbell L, Barar J, Connell D, Akhtar S, Gumbleton M. Evaluation of the immortalised mouse brain capillary endothelial cell line, b.End3, as an in vitro blood-brain barrier model for drug uptake and transport studies. Brain Res. 2003; 990:95–112. [PubMed: 14568334]
26. Eigenmann DE, Xue G, Kim KS, Moses AV, Hamburger M, Oufir M. Comparative study of four immortalized human brain capillary endothelial cell lines, hCMEC/D3, hBMEC, TY10, and BB19, and optimization of culture conditions, for an in vitro blood-brain barrier model for drug permeability studies. Fluids Barriers CNS. 2013; 10:33. [PubMed: 24262108]

Author Manuscript Author Manuscript Author Manuscript Author Manuscript

27. Cooray HC, Shahi S, Cahn AP, van Veen HW, Hladky SB, Barrand MA. Modulation of p-glycoprotein and breast cancer resistance protein by some prescribed corticosteroids. Eur J Pharmacol. 2006; 531:25–33. [PubMed: 16442095]
28. Stamatovic SM, Dimitrijevic OB, Keep RF, Andjelkovic AV. Protein kinase Calpha-RhoA cross-talk in CCL2-induced alterations in brain endothelial permeability. J Biol Chem. 2006; 281:8379–8388. [PubMed: 16439355]
29. Zhang JH, Chung TD, Oldenburg KR. A Simple Statistical Parameter for Use in Evaluation and Validation of High Throughput Screening Assays. J Biomol Screen. 1999; 4:67–73. [PubMed: 10838414]
30. Wu, G. Assay development : fundamentals and practices. Wiley; Hoboken, N.J: 2010.
31. Varma H, Lo DC, Stockwell BR. High-Throughput and High-Content Screening for Huntington's Disease Therapeutics. 2011
32. Chung N, Zhang XD, Kreamer A, Locco L, Kuan PF, Bartz S, Linsley PS, Ferrer M, Strulovici B. Median absolute deviation to improve hit selection for genome-scale RNAi screens. J Biomol Screen. 2008; 13:149–158. [PubMed: 18216396]
33. Qosa H, LeVine H 3rd, Keller JN, Kaddoumi A. Mixed oligomers and monomeric amyloid-beta disrupts endothelial cells integrity and reduces monomeric amyloid-beta transport across hCMEC/D3 cell line as an in vitro blood-brain barrier model. Biochim Biophys Acta. 2014; 1842:1806–1815. [PubMed: 24997450]
34. Qosa H, Batarseh YS, Mohyeldin MM, El Sayed KA, Keller JN, Kaddoumi A. Oleocanthal Enhances Amyloid-beta Clearance from the Brains of TgSwDI Mice and in Vitro across a Human Blood-Brain Barrier Model. ACS Chem Neurosci. 2015
35. Qosa H, Abuasal BS, Romero IA, Weksler B, Couraud PO, Keller JN, Kaddoumi A. Differences in amyloid-beta clearance across mouse and human blood-brain barrier models: kinetic analysis and mechanistic modeling. Neuropharmacology. 2014; 79:668–678. [PubMed: 24467845]
36. Hartmann C, Zozulya A, Wegener J, Galla HJ. The impact of glia-derived extracellular matrices on the barrier function of cerebral endothelial cells: an in vitro study. Exp Cell Res. 2007; 313:1318–1325. [PubMed: 17346702]
37. Tilling T, Engelbertz C, Decker S, Korte D, Huwel S, Galla HJ. Expression and adhesive properties of basement membrane proteins in cerebral capillary endothelial cell cultures. Cell Tissue Res. 2002; 310:19–29. [PubMed: 12242480]
38. Wuest DM, Wing AM, Lee KH. Membrane configuration optimization for a murine in vitro blood-brain barrier model. J Neurosci Methods. 2013; 212:211–221. [PubMed: 23131353]
39. Hulper P, Veszelka S, Walter FR, Wolburg H, Fallier-Becker P, Piontek J, Blasig IE, Lakomek M, Kugler W, Deli MA. Acute effects of short-chain alkylglycerols on blood-brain barrier properties of cultured brain endothelial cells. Br J Pharmacol. 2013; 169:1561–1573. [PubMed: 23617601]
40. Kashiwamura Y, Sano Y, Abe M, Shimizu F, Haruki H, Maeda T, Kawai M, Kanda T. Hydrocortisone enhances the function of the blood-nerve barrier through the up-regulation of claudin-5. Neurochem Res. 2011; 36:849–855. [PubMed: 21293925]
41. Forster C, Burek M, Romero IA, Weksler B, Couraud PO, Drenckhahn D. Differential effects of hydrocortisone and TNFalpha on tight junction proteins in an in vitro model of the human blood-brain barrier. J Physiol. 2008; 586:1937–1949. [PubMed: 18258663]
42. Abbott NJ, Patabendige AA, Dolman DE, Yusof SR, Begley DJ. Structure and function of the blood-brain barrier. Neurobiol Dis. 2010; 37:13–25. [PubMed: 19664713]
43. Winkler EA, Bell RD, Zlokovic BV. Central nervous system pericytes in health and disease. Nat Neurosci. 2011; 14:1398–1405. [PubMed: 22030551]
44. Bell RD, Winkler EA, Sagare AP, Singh I, LaRue B, Deane R, Zlokovic BV. Pericytes control key neurovascular functions and neuronal phenotype in the adult brain and during brain aging. Neuron. 2010; 68:409–427. [PubMed: 21040844]
45. Sofroniew MV, Vinters HV. Astrocytes: biology and pathology. Acta Neuropathol. 2010; 119:7–35. [PubMed: 20012068]
46. Fernández-Klett F, Potas JR, Hilpert D, Blazej K, Radke J, Huck J, Engel O, Stenzel W, Genové G, Priller J. Early loss of pericytes and perivascular stromal cell-induced scar formation after stroke. J Cereb Blood Flow Metab. 2013; 33:428–439. [PubMed: 23250106]

Author Manuscript Author Manuscript Author Manuscript Author Manuscript

47. Price TO, Eranki V, Banks WA, Ercal N, Shah GN. Topiramate treatment protects blood-brain barrier pericytes from hyperglycemia-induced oxidative damage in diabetic mice. Endocrinology. 2012; 153:362–372. [PubMed: 22109883]
48. Dore-Duffy P, Owen C, Balabanov R, Murphy S, Beaumont T, Rafols JA. Pericyte migration from the vascular wall in response to traumatic brain injury. Microvasc Res. 2000; 60:55–69. [PubMed: 10873515]
49. Wilhelmus MM, Otte-Holler I, van Triel JJ, Veerhuis R, Maat-Schieman ML, Bu G, de Waal RM, Verbeek MM. Lipoprotein receptor-related protein-1 mediates amyloid-beta-mediated cell death of cerebrovascular cells. Am J Pathol. 2007; 171:1989–1999. [PubMed: 18055545]
50. Sagare AP, Bell RD, Zhao Z, Ma Q, Winkler EA, Ramanathan A, Zlokovic BV. Pericyte loss influences Alzheimer-like neurodegeneration in mice. Nat Commun. 2013; 4:2932. [PubMed: 24336108]
51. Watanabe T, Dohgu S, Takata F, Nishioku T, Nakashima A, Futagami K, Yamauchi A, Kataoka Y. Paracellular barrier and tight junction protein expression in the immortalized brain endothelial cell lines bEND.3, bEND.5 and mouse brain endothelial cell 4. Biol Pharm Bull. 2013; 36:492–495. [PubMed: 23449334]
52. Yuan W, Li G, Gil ES, Lowe TL, Fu BM. Effect of surface charge of immortalized mouse cerebral endothelial cell monolayer on transport of charged solutes. Ann Biomed Eng. 2010; 38:1463–1472. [PubMed: 20087768]
53. Jo DG, Arumugam TV, Woo HN, Park JS, Tang SC, Mughal M, Hyun DH, Park JH, Choi YH, Gwon AR, Camandola S, Cheng A, Cai H, Song W, Markesbery WR, Mattson MP. Evidence that gamma-secretase mediates oxidative stress-induced beta-secretase expression in Alzheimer's disease. Neurobiol Aging. 2010; 31:917–925. [PubMed: 18687504]
54. Malo N, Hanley JA, Cerquozzi S, Pelletier J, Nadon R. Statistical practice in high-throughput screening data analysis. Nat Biotechnol. 2006; 24:167–175. [PubMed: 16465162]
55. McClung HJ, Sloan HR, Powers P, Merola AJ, Murray R, Kerzner B, Pollack JD. Early changes in the permeability of the blood-brain barrier produced by toxins associated with liver failure. Pediatr Res. 1990; 28:227–231. [PubMed: 2235119]
56. Appleby BS, Cummings JL. Discovering new treatments for Alzheimer's disease by repurposing approved medications. Curr Top Med Chem. 2013; 13:2306–2327. [PubMed: 24059463]
57. Corbett A, Ballard C. Is a potential Alzheimer's therapy already in use for other conditions? Can medications for hypertension, diabetes and acne help with the symptoms? Expert Opin Investig Drugs. 2013; 22:941–943.
58. Shehata IA, Ballard JR, Casper AJ, Hennings LJ, Cressman E, Ebbini ES. High-intensity focused ultrasound for potential treatment of polycystic ovary syndrome: toward a noninvasive surgery. Fertil Steril. 2014; 101:545–551. [PubMed: 24290002]
59. Hardy J. The amyloid hypothesis for Alzheimer's disease: a critical reappraisal. J Neurochem. 2009; 110:1129–1134. [PubMed: 19457065]
60. Iwata N, Tsubuki S, Takaki Y, Watanabe K, Sekiguchi M, Hosoki E, Kawashima-Morishima M, Lee HJ, Hama E, Sekine-Aizawa Y, Saido TC. Identification of the major Abeta1-42-degrading catabolic pathway in brain parenchyma: suppression leads to biochemical and pathological deposition. Nat Med. 2000; 6:143–150. [PubMed: 10655101]
61. Silverberg GD, Mayo M, Saul T, Rubenstein E, McGuire D. Alzheimer's disease, normal-pressure hydrocephalus, and senescent changes in CSF circulatory physiology: a hypothesis. Lancet Neurol. 2003; 2:506–511. [PubMed: 12878439]
62. Zlokovic BV, Yamada S, Holtzman D, Ghiso J, Frangione B. Clearance of amyloid beta-peptide from brain: transport or metabolism? Nat Med. 2000; 6:718–719.
63. Cirrito JR, Deane R, Fagan AM, Spinner ML, Parsadanian M, Finn MB, Jiang H, Prior JL, Sagare A, Bales KR, Paul SM, Zlokovic BV, Piwnica-Worms D, Holtzman DM. P-glycoprotein deficiency at the blood-brain barrier increases amyloid-beta deposition in an Alzheimer disease mouse model. J Clin Invest. 2005; 115:3285–3290. [PubMed: 16239972]
64. Shibata M, Yamada S, Kumar SR, Calero M, Bading J, Frangione B, Holtzman DM, Miller CA, Strickland DK, Ghiso J, Zlokovic BV. Clearance of Alzheimer's amyloid-ss(1-40) peptide from

Author Manuscript Author Manuscript Author Manuscript Author Manuscript

brain by LDL receptor-related protein-1 at the blood-brain barrier. J Clin Invest. 2000; 106:1489–1499. [PubMed: 11120756]

65. Giannoni P, Arango-Lievano M, Neves ID, Rousset MC, Baranger K, Rivera S, Jeanneteau F, Claeysen S, Marchi N. Cerebrovascular pathology during the progression of experimental Alzheimer's disease. Neurobiol Dis. 2016; 88:107–117. [PubMed: 26774030]
66. Park L, Zhou J, Zhou P, Pistick R, El Jamal S, Younkin L, Pierce J, Arreguin A, Anrather J, Younkin SG, Carlson GA, McEwen BS, Iadecola C. Innate immunity receptor CD36 promotes cerebral amyloid angiopathy. Proc Natl Acad Sci U S A. 2013; 110:3089–3094. [PubMed: 23382216]
67. Paul J, Strickland S, Melchor JP. Fibrin deposition accelerates neurovascular damage and neuroinflammation in mouse models of Alzheimer's disease. J Exp Med. 2007; 204:1999–2008. [PubMed: 17664291]
68. Carrano A, Hoozemans JJ, van der Vies SM, Rozemuller AJ, van Horssen J, de Vries HE. Amyloid Beta induces oxidative stress-mediated blood-brain barrier changes in capillary amyloid angiopathy. Antioxid Redox Signal. 2011; 15:1167–1178. [PubMed: 21294650]
69. Hartz AM, Bauer B, Soldner EL, Wolf A, Boy S, Backhaus R, Mihaljevic I, Bogdahn U, Klunemann HH, Schuierer G, Schlachetzki F. Amyloid-beta contributes to blood-brain barrier leakage in transgenic human amyloid precursor protein mice and in humans with cerebral amyloid angiopathy. Stroke. 2012; 43:514–523. [PubMed: 22116809]
70. Tai LM, Holloway KA, Male DK, Loughlin AJ, Romero IA. Amyloid-beta-induced occludin down-regulation and increased permeability in human brain endothelial cells is mediated by MAPK activation. J Cell Mol Med. 2010; 14:1101–1112. [PubMed: 19438816]
71. Zlokovic BV. Neurovascular pathways to neurodegeneration in Alzheimer's disease and other disorders. Nat Rev Neurosci. 2011; 12:723–738. [PubMed: 22048062]
72. Dorr A, Sahota B, Chinta LV, Brown ME, Lai AY, Ma K, Hawkes CA, McLaurin J, Stefanovic B. Amyloid-beta-dependent compromise of microvascular structure and function in a model of Alzheimer's disease. Brain. 2012; 135:3039–3050. [PubMed: 23065792]
73. Mawuenyega KG, Sigurdson W, Ovod V, Munsell L, Kasten T, Morris JC, Yarasheski KE, Bateman RJ. Decreased clearance of CNS beta-amyloid in Alzheimer's disease. Science. 2010; 330:1774. [PubMed: 21148344]
74. Chugh Y, Saha N, Sankaranarayanan A, Sharma PL. Memory enhancing effects of granisetron (BRL 43694) in a passive avoidance task. Eur J Pharmacol. 1991; 203:121–123. [PubMed: 1665786]
75. Ban, Ju Yeon; Seong, Yeon Hee. Blockade of 5-HT(3) receptor with MDL 72222 and Y 25130 reduces beta-amyloid protein (25–35)-induced neurotoxicity in cultured rat cortical neurons. Eur J Pharmacol. 2005; 520:12–21. [PubMed: 16150439]
76. Javadi-Paydar M, Zakeri M, Norouzi A, Rastegar H, Mirazi N, Dehpour AR. Involvement of nitric oxide in granisetron improving effect on scopolamine-induced memory impairment in mice. Brain Res. 2012; 1429:61–71. [PubMed: 21875703]
77. in t' Veld BA, Ruitenberg A, Hofman A, Launer LJ, van Duijn CM, Stijnen T, Breteler MM, Stricker BH. Nonsteroidal antiinflammatory drugs and the risk of Alzheimer's disease. N Engl J Med. 2001; 345:1515–1521. [PubMed: 11794217]
78. Yip AG, Green RC, Huyck M, Cupples LA, Farrer LA. Mirage Study Group. Nonsteroidal anti-inflammatory drug use and Alzheimer's disease risk: the MIRAGE study. BMC Geriatr. 2005; 5:2. [PubMed: 15647106]
79. Wang J, Tan L, Wang HF, Tan CC, Meng XF, Wang C, Tang SW, Yu JT. Anti-inflammatory drugs and risk of Alzheimer's disease: an updated systematic review and meta-analysis. J Alzheimers Dis. 2015; 44:385–396. [PubMed: 25227314]
80. Choi JK, Carreras I, Aytan N, Jenkins-Sahlin E, Dedeoglu A, Jenkins BG. The effects of aging, housing and ibuprofen treatment on brain neurochemistry in a triple transgene Alzheimer's disease mouse model using magnetic resonance spectroscopy and imaging. Brain Res. 2014; 1590:85–96. [PubMed: 25301691]

Author Manuscript Author Manuscript Author Manuscript Author Manuscript

81. Yan Q, Zhang J, Liu H, Babu-Khan S, Vassar R, Biere AL, Citron M, Landreth G. Anti-inflammatory drug therapy alters beta-amyloid processing and deposition in an animal model of Alzheimer's disease. J Neurosci. 2003; 23:7504–7509. [PubMed: 12930788]

82. Pasinetti GM. From epidemiology to therapeutic trials with anti-inflammatory drugs in Alzheimer's disease: the role of NSAIDs and cyclooxygenase in beta-amyloidosis and clinical dementia. J Alzheimers Dis. 2002; 4:435–445. [PubMed: 12446975]

83. Szekely CA, Zandi PP. Non-steroidal anti-inflammatory drugs and Alzheimer's disease: the epidemiological evidence. CNS Neurol Disord Drug Targets. 2010; 9:132–139. [PubMed: 20205647]

84. ADAPT-FS Research Group. Follow-up evaluation of cognitive function in the randomized Alzheimer's Disease Anti-inflammatory Prevention Trial and its Follow-up Study. Alzheimers Dement. 2015; 11:216–225. [PubMed: 25022541]

Author Manuscript Author Manuscript Author Manuscript Author Manuscript

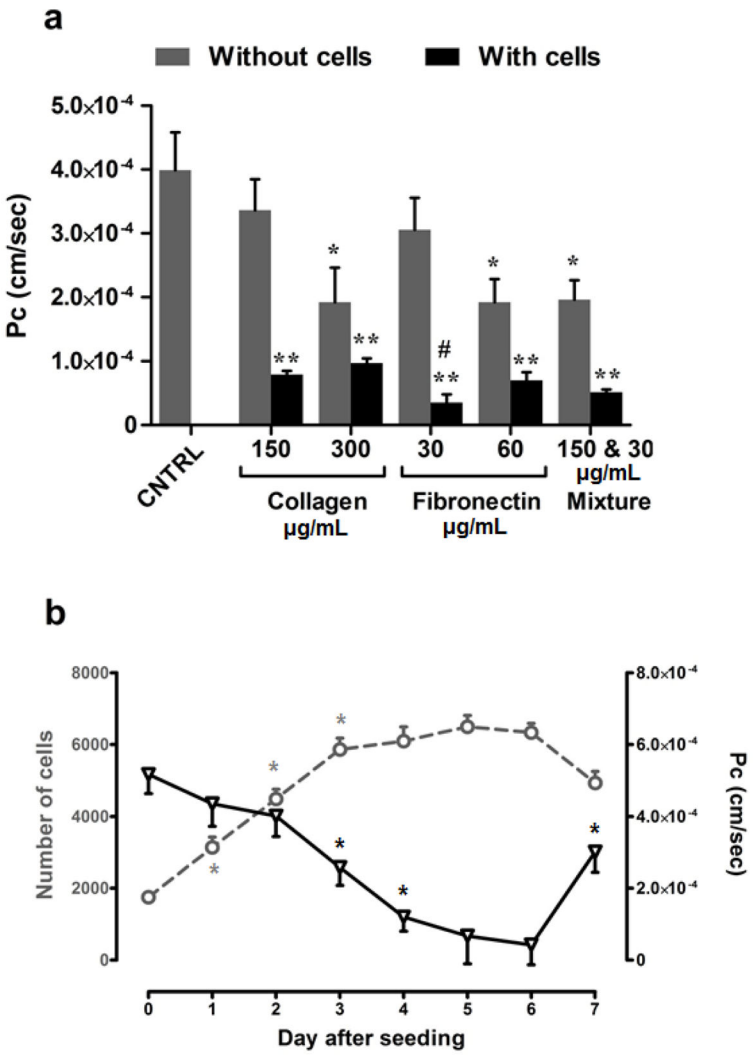

Figure 1.

Model optimization. (a) Optimization of basement membrane substitute. LY permeation across bEnd3 monolayer grown on the top of polycarbonate transwell coated with 150 or 300 µg/ml rat-tail collagen type I, 30 or 60 µg/ml fibronectin, and a mixture of 150 µg/ml rat-tail collagen and 30 µg/ml fibronectin. LY permeation was represented as permeation coefficient (Pc). Compared to other tested coatings, in the presence of cells, fibronectin at 30 µg/ml offered the lowest Pc value indicative of restricted transport due to formation of a tight monolayer, and in the absence of cells fibronectin did not act as a barrier to LY transport. Data represented as mean±SEM for 9 replicates from 3 independent experiments. * $P<0.05$, ** $P<0.01$ values compared to control, # $P<0.05$ compared to collagen at 150 µg/ml.**(b)** Time-dependent changes in bEnd3 cells growth (open circles) and LY permeation across the bEnd3 cells-based BBB model (open triangles). Growth pattern of bEnd3 cells after seeding indicates formation of confluent monolayer on day 3 post-seeding. On the other hand, LY permeation started to decrease from day 1 and continue to decrease until day 4 where it remains contestant until day 6. LY permeation change indicates formation of tight junction

between cells in confluent bEnd3 monolayer. Data represented as mean±SEM for 6 replicates from 2 independent experiments (* $p < 0.05$).

Author Manuscript Author Manuscript Author Manuscript Author Manuscript

Author Manuscript Author Manuscript Author Manuscript Author Manuscript

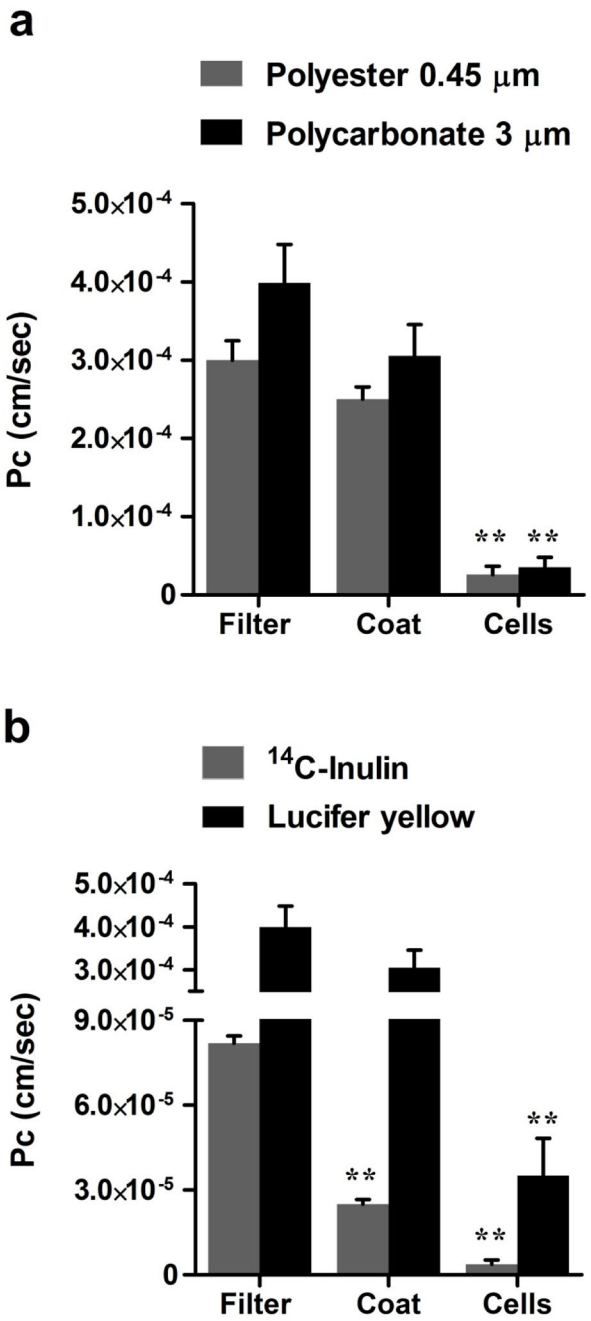

Figure 2.

Assay validation. (a) Comparison of LY permeation coefficient across bEnd3 monolayer grown on the top of polycarbonate transwell of 3 μm pore size and polyester transwell of 0.45 pore size. The results showed no differences between LY permeation coefficients across two bEnd3 monolayer grown on either supporting membrane. (b) Comparison of LY permeation coefficient to that of ^{14}C-inulin. Inulin showed significantly lower permeation coefficient compared to LY. Data represented as mean±SEM for 6 replicates from 2 independent experiments. * $P<0.05$, ** $P<0.01$ values compared to filter.

Author Manuscript Author Manuscript Author Manuscript Author Manuscript

a

	Mannitol	Hydrocortisone
Z′ factor	0.78±0.08 (0.62-0.88)	0.3±0.11 (0.15-0.5)
S/N	34.20±6.50 (29-43)	11.00±2.20 (8-14)
S/B	2.76±0.21 (2.3-3)	0.64±0.17 (0.3-0.8)
# of plates screened	125	125
# of compounds screened	1280	1280
# of hits selected	62	50

b

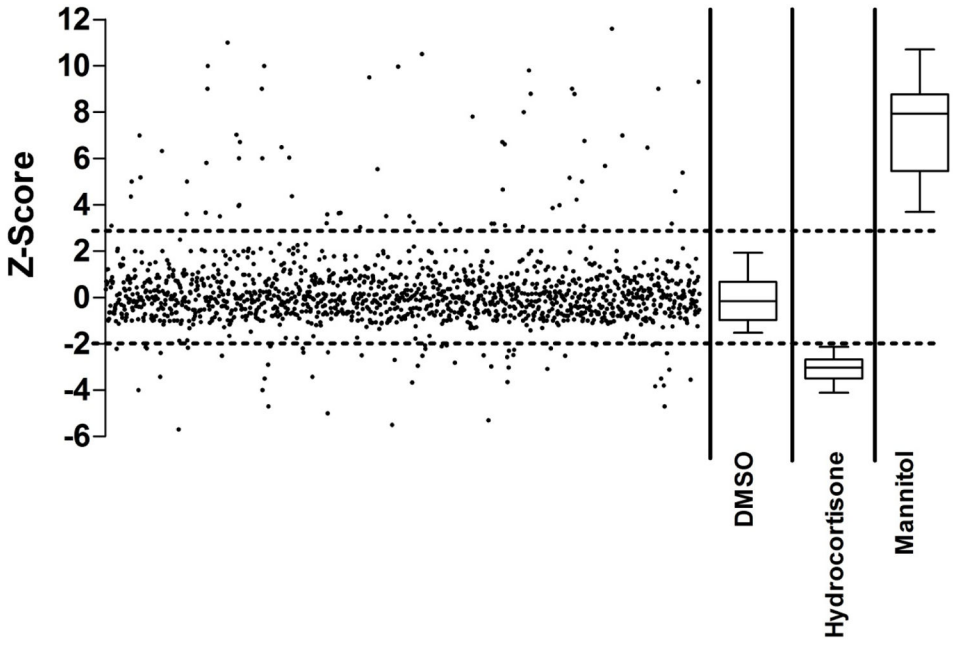

Figure 3.

(a) Performance of bEnd3 cells-based BBB model in the HTS for disruptors and enhancers of the barrier function. (b) Screening of 1280 compounds of Sigma LOPAC[1280] library for their effect on the integrity of bEnd3 cells-based BBB model. LY permeation coefficient of each compound was normalized to the plate median and MAD to obtain a standardized *z*-score value that was plotted for each compound. The upper dotted line represents the *z*-score cutoff corresponding to 3 MAD above the plate median. z-Score values above the upper dotted line represent compounds which disrupt the barrier function of the in vitro model. The lower dotted line represents z-score cutoff corresponding to 2 MADs below the plate median. z-Score values below the lower dotted line represent compounds enhancers of the barrier function of the BBB model. DMSO (negative control, 0.1%), hydrocortisone (positive control for enhancers, 10 μM) and Mannitol (positive control for disruptors, 1.4 M) were plotted as box plots to show the model performance.

Author Manuscript Author Manuscript Author Manuscript Author Manuscript

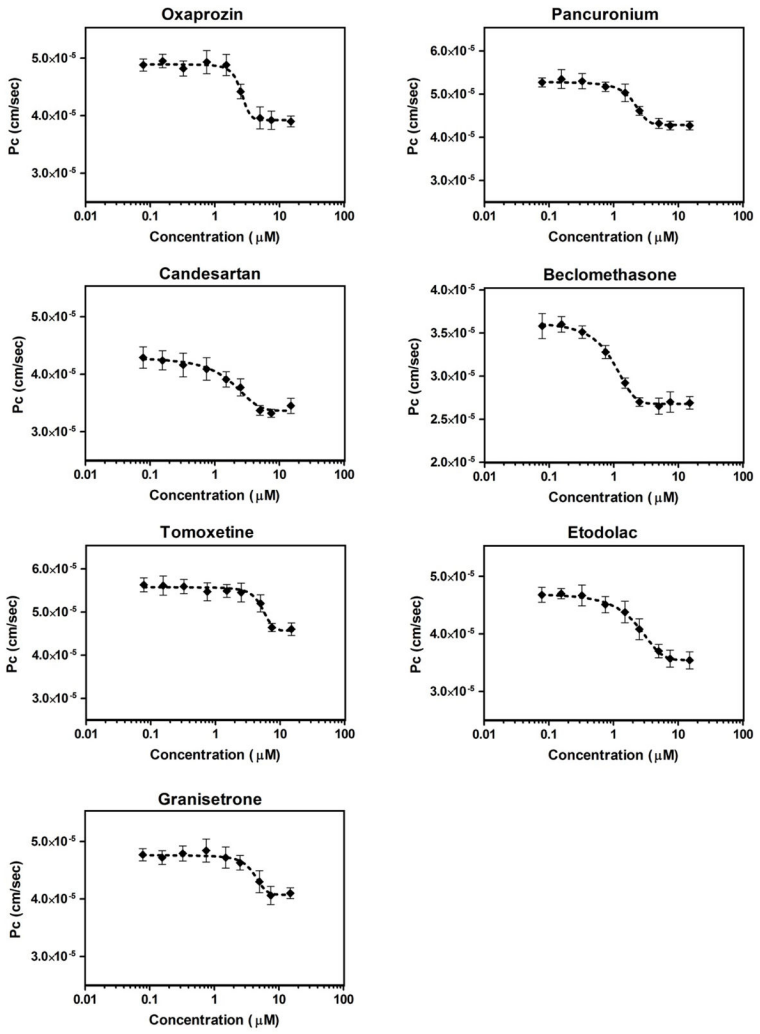

Figure 4.

Hits validation. 10-Point concentration-response curves of the seven FDA approved drugs that showed significant enhancement in the barrier function of the bEnd3 cells-based BBB model. The drugs were tested in the concentration range 0.065–20 μM to calculate compounds EC_{50}s. The 10th point (20 μM) was eliminated from the curves due to toxicity. Data represent mean±SEM, n = 6 for each concentration.

Author Manuscript Author Manuscript Author Manuscript Author Manuscript

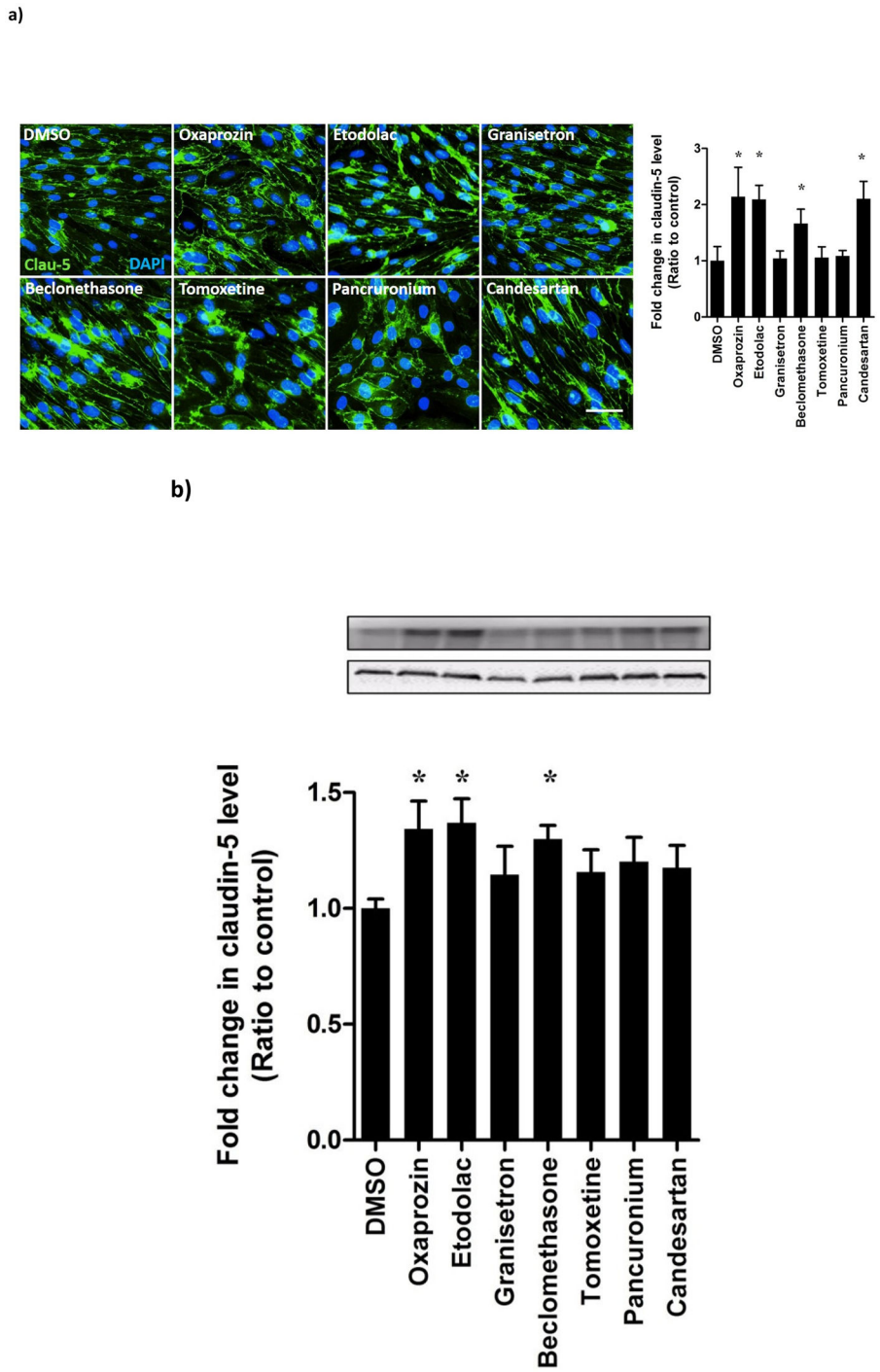

Figure 5.

(a) Representative images of claudin-5 in bEnd3 cells monolayers treated with hit FDA drugs showing localization and expression of claudin-5 in the membrane of bEnd3 cells (scale bar = 50 μm) (b) Representative blots and densitometry analysis for the effect of hit FDA drugs treatment on cluadin-5 expression determined by Western blot. Data represented as mean±SEM from 3 independent experiments. * $P<0.05$.

Author Manuscript Author Manuscript Author Manuscript Author Manuscript

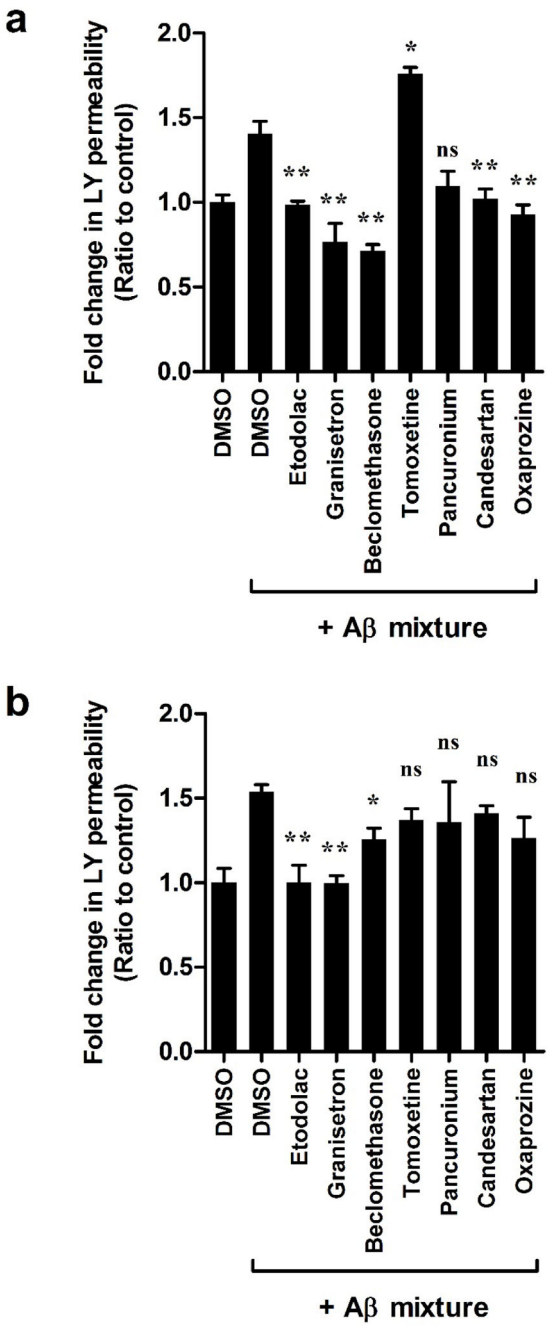

Figure 6.

Effect of the hit FDA drugs on rectifying the attenuated integrity of bEnd3 cells-based BBB model (a), and the human hCMEC/D3 cells-based BBB model (b) by Aβ mixture (100 nM $A\beta_{40}$ monomers and 200 nM $A\beta_{42}$ oligomers with bEnd3 cells; 50 nM $A\beta_{40}$ monomers and 100 nM $A\beta_{42}$ oligomers with hCMEC/D3 cells). Data represented as mean±SEM for 6 replicates from 2 independent experiments. * $P<0.05$, ** $P<0.01$ values compared to filter.

Author Manuscript Author Manuscript Author Manuscript Author Manuscript

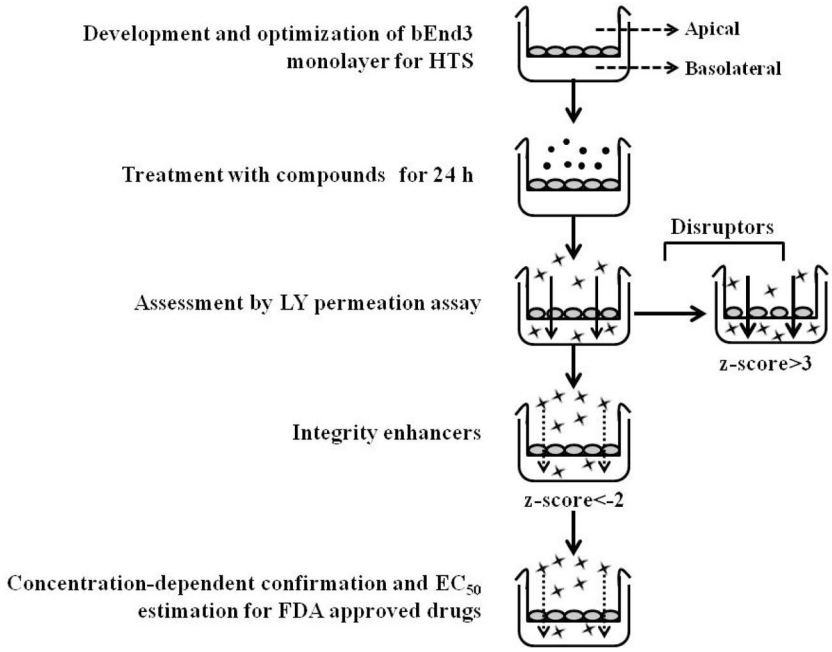

Scheme 1.

Schematic presentation of bEnd3 cells-based BBB model optimization and application.

Author Manuscript Author Manuscript Author Manuscript Author Manuscript

Table 1

Description and EC_{50} values of FDA approved drugs obtained from primary and secondary screenings that showed significant enhancement in the barrier function of bEnd3 monolayer.

Drug	Description[a]	EC_{50} (μM)
Beclomethasone	Anti-inflammatory glucocorticoid	0.76
Candesartan	Angiotensin II receptor antagonist	1.17
Pancuronium	Neuromuscular blocking agent; skeletal muscle relaxant	2.24
Etodolac	Non-steroidal anti-inflammatory drug (NSAID)	2.32
Oxaprozin	Non-steroidal anti-inflammatory drug (NSAID)	3.14
Tomoxetine	Norepinephrine reuptake blocker	3.86
Granisetron	Serotonin 5-HT3 receptor antagonist and antiemetic	4.56

[a]Sigma Aldrich Website, http://www.sigmaaldrich.com/chemistry/drug-discovery/validation-libraries/lopac1280-navigator.html.

Author Manuscript Author Manuscript Author Manuscript Author Manuscript

Table 2

FDA approved drugs that caused significant disruption in the barrier function of the bEnd3 cells-based BBB model from the primary screen.

Drug	Description[a]
Bexarotene	Highly selective retinoid X receptor (RXR) agonist
Colchicine	Prevents tubulin polymerization
Demeclocycline	Tetracycline antibiotic; interferes with protein synthesis
Felodipine	L-type calcium channel blocker
Idarubicin	Antineoplastic
Oxybutynin	Muscarinic acetylcholine receptor antagonist
Reserpine	Inhibits vesicular catecholine and serotonin uptake.
Topotecan	Topoisomerase I (topo-I) inhibitor
Vincristine	Inhibitor of microtubule assembly
Vinblastine	Inhibitor of microtubule assembly

[a]Sigma Aldrich Website, http://www.sigmaaldrich.com/chemistry/drug-discovery/validation-libraries/lopac1280-navigator.html.